Temperature Change on the Antarctic Peninsula Linked to the Tropical Pacific*

QINGHUA DING AND ERIC J. STEIG

Department of Earth and Space Sciences and Quaternary Research Center, University of Washington, Seattle, Washington

(Manuscript received 12 October 2012, in final form 16 February 2013)

ABSTRACT

Significant summer warming over the eastern Antarctic Peninsula in the last 50 years has been attributed to a strengthening of the circumpolar westerlies, widely believed to be anthropogenic in origin. On the western side of the peninsula, significant warming has occurred mainly in austral winter and has been attributed to the reduction of sea ice. The authors show that austral fall is the only season in which spatially extensive warming has occurred on the Antarctic Peninsula. This is accompanied by a significant reduction of sea ice cover off the west coast. In winter and spring, warming is mainly observed on the west side of the peninsula. The most important large-scale forcing of the significant widespread warming trend in fall is the extratropical Rossby wave train associated with tropical Pacific sea surface temperature anomalies. Winter and spring warming on the western peninsula reflects the persistence of sea ice anomalies arising from the tropically forced atmospheric circulation changes in austral fall.

1. Introduction

Surface temperature changes in Antarctica over the last 50 years exhibit strong seasonality and spatial complexity, with significant increases of annual mean temperature on the Antarctic Peninsula (AP) and West Antarctica but little change across East Antarctica (Comiso 2000; Marshall et al. 2002; Turner et al. 2005; Chapman and Walsh 2007; Monaghan and Bromwich 2008; Monaghan et al. 2008; Steig et al. 2009; Schneider et al. 2012a; Orsi et al. 2012; Fogt et al. 2012; Bromwich et al. 2013; Steig and Orsi 2013). In the peninsula region, the warming on the west side is greatest in austral winter, while on the east side the warming is greatest in summer. In some locations on the western AP, the annual-mean warming trend reaches 0.5°C decade^{-1}, which is substantially larger than global mean warming and ranks among the fastest warming rates on the planet (Vaughan et al. 2003). Significant changes to ecosystems in this area are among the known impacts of this warming (Trivelpiece et al. 2011). On the eastern side of the AP, successive loss of ice shelves has occurred in response to summer surface warming (Van den Broeke 2005).

The summer warming over the eastern AP in recent decades has been attributed to a trend of atmospheric circulation toward the positive phase of the southern annular mode (SAM) (Thompson and Solomon 2002; Gillett et al. 2006; Marshall et al. 2006; Marshall 2007), the dominant pattern of Southern Hemisphere (SH) circulation variability (Thompson and Wallace 2000). There is evidence that the observed trend in the SAM index during austral summer is the result of anthropogenic increases in greenhouse gas concentrations and depletion of stratospheric ozone (Thompson and Solomon 2002; Gillett and Thompson 2003; Marshall et al. 2004; Shindell and Schmidt 2004; Miller et al. 2006; Arblaster and Meehl 2006; Fogt et al. 2009; Thompson et al. 2011). The positive SAM trend may induce warming on the east side of the peninsula through a feedback between increased westerlies and local topography (van Lipzig et al. 2008; Orr et al. 2008). Thus, the recent warming trend on the eastern AP reflects the impact of anthropogenic forcing on the SH high-latitude circulation. These arguments do not account for the warming on the west AP during winter, which is commonly attributed to the decreasing trend of sea ice in the Bellingshausen Sea off the west coast of the peninsula (Jacobs and Comiso 1997). It has been suggested that sea ice variability in the Bellingshausen Sea is sensitive to the SAM and El Niño–Southern Oscillation

* Supplemental information related to this paper is available at the Journals Online website: http://dx.doi.org/10.1175/JCLI-D-12-00729.s1.

Corresponding author address: Qinghua Ding, Department of Earth and Space Sciences and Quaternary Research Center, University of Washington, 4000 15th Av. NE, Seattle, WA 98195.
E-mail: qinghua@uw.edu

DOI: 10.1175/JCLI-D-12-00729.1

FIG. 1. Locations of the eight weather stations used for this study. Bellingshausen and Marsh are two different stations but with almost the same longitude/latitude. Faraday station is now operated by the Ukrainian Antarctic Program and is referred to as Faraday/Vernadsky.

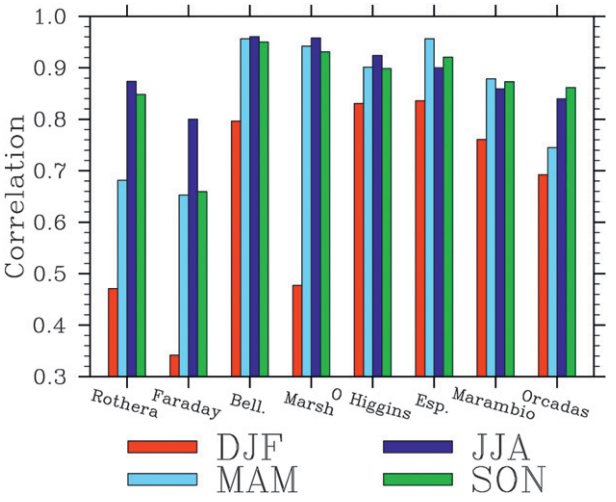

FIG. 2. Correlation of seasonal mean temperature at AP weather stations with the APT time series (mean of eight stations) in the corresponding season. The sequence of stations on the abscissa is based on the longitude of each site (from the westernmost to the easternmost). All correlations shown are significant at 95% confidence level (±0.35), except one for Faraday during DJF.

(ENSO) variability (Liu et al. 2004; Stammerjohn et al. 2008), but the cause of the long-term sea ice reduction trend remains an open question (Vaughan et al. 2003; Sigmond and Fyfe 2010; Holland and Kwok 2012).

An important link between tropical SST anomalies and circulation variability in the high latitudes of the SH has been recognized for decades (Karoly 1989; Liu et al. 2002; Grassi et al. 2005; Fogt et al. 2009). In particular, SST variability in the tropical Pacific is strongly linked to the circulation variability adjacent to the AP and continental West Antarctica, through the generation of a large-scale atmospheric wave train (Marshall and King 1998; Yuan and Martinson 2000; Renwick 2002; Yuan 2004; Fogt and Bromwich 2006; Lachlan-Cope and Connolley 2006; Ding et al. 2011; Fogt et al. 2011; Steig et al. 2012; Schneider et al. 2012a,b; Ding et al. 2012; Okumura et al. 2012; Bromwich et al. 2013). This motivates examination of the role of tropical SST variability in influencing the observed trend of AP temperatures and sea ice conditions.

2. Methods

a. Data

We use data from the eight long weather stations on the AP to examine peninsula-wide temperature variability (Fig. 1). We restrict the analysis to the most recent 31 years (1979–2009), during which atmospheric reanalysis data for the SH polar region are most reliable (Bromwich et al. 2007; Bracegirdle and Marshall 2012). Monthly near-surface temperature from eight stations in the AP region was obtained from the Antarctic Reference Antarctic Data for Environmental Research (READER) project (Turner et al. 2005). These eight stations were chosen because they have monthly data for at least 95% of the 31-yr period examined. The locations of these eight stations are roughly uniformly distributed along the coast of the AP (Fig. 1). A cross-correlation calculation between temperature from any pair of the eight stations shows that in summer, temperature on the west side of the peninsula (Faraday/Vernadsky and Rothera, Antarctica) is largely independent from temperature variability on the east side (see Table S1 in the supplemental material). In the other three seasons, however, temperatures at all AP stations vary together. We construct a time series of AP temperature (APT) by averaging monthly temperature from all eight stations. APT is highly correlated with temperature at each individual station in all seasons except summer (Fig. 2). Correlation of APT with surface temperature in the European Centre for Medium-Range Weather Forecasts (ECMWF) Interim Re-Analysis (ERA-Interim; Dee et al. 2011) shows that APT is representative of the temperature variability across most of the AP in fall [March–May (MAM)], winter [June–August (JJA)], and spring [September–November (SON)] (Fig. 3), and thus provides a meaningful measure of peninsula-wide temperature change in those seasons. To separately consider the temperature variability on each side of the peninsula, the

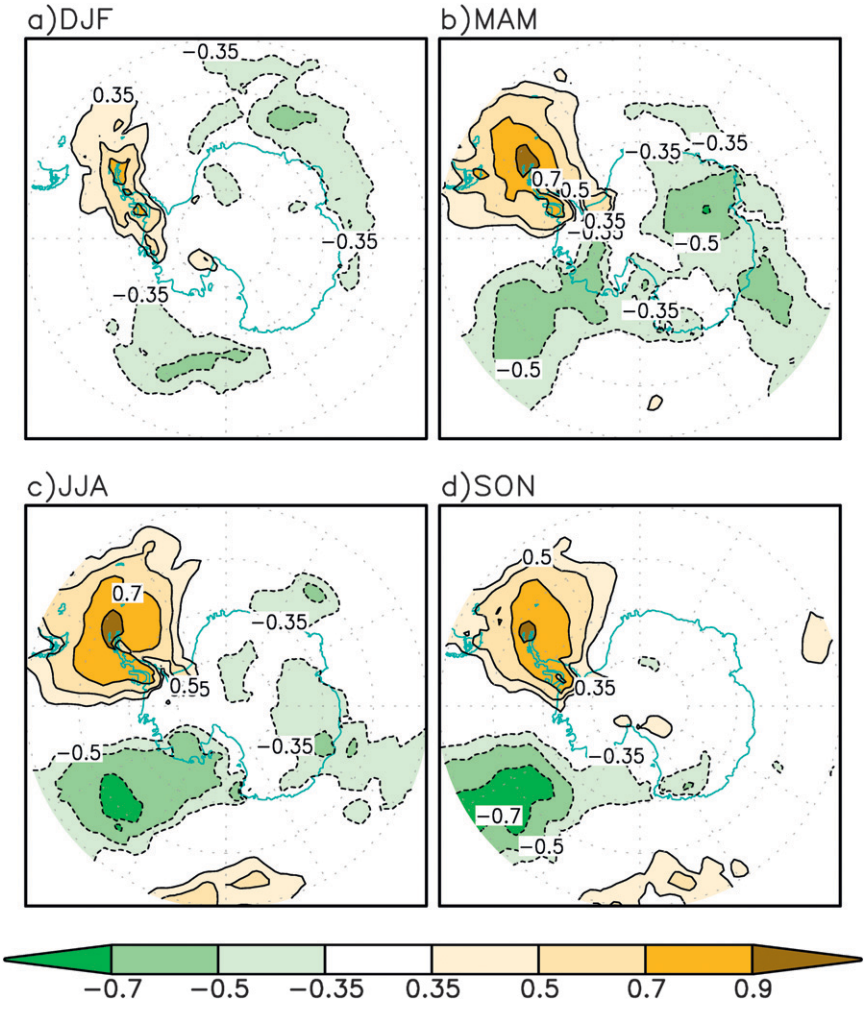

FIG. 3. Correlation of seasonal mean APT with ERA-Interim surface air temperature in the corresponding season: (a) DJF, (b) MAM, (c) JJA, and (d) SON. Only significant correlation (above 95% confidence level: ±0.35) are displayed.

mean of temperatures from Faraday/Vernadsky and Rothera, which are located on the west coast of peninsula, are defined as the W-APT. The mean of temperatures from the remaining six stations, which are located on the east side, are defined as the E-APT.

Atmospheric circulation and surface temperature data are from the 1979–2009 ERA-Interim (Dee et al. 2011). Sea surface temperature data are from the Extended Reconstructed SST, version 3 (ERSSTv3), dataset (Smith et al. 2008) and sea ice data are from the Hadley Centre Sea Ice and Sea Surface Temperature dataset (HadISST; Rayner et al. 2003). The spatial field of surface temperature is also derived from thermal infrared channels of the Advanced Very High Resolution Radiometer (AVHRR) satellite (Comiso 2000) and Modern-Era Retrospective Analysis for Research and Applications (MERRA; Rienecker et al. 2011), which are largely independent of the ERA-Interim datasets. It should be noted that because the reliable data for the SH polar region is short, the term ''trend'' used in the following refer to any low-frequency variability distinct from the interannual variability; it does not necessarily imply a long-term trend, but may simply reflect decadal variability.

b. Method

To examine the tropical connection of the AP temperature, we use maximum covariance analysis (MCA; Bretherton et al. 1992) to capture the dominant coupled modes between surface temperature on the AP and tropical SST. The MCA is achieved by singular value decomposition of the temporal covariance matrix, using equal area (square root of cosine of latitude) weighting. The pairs of singular vectors describe the spatial patterns

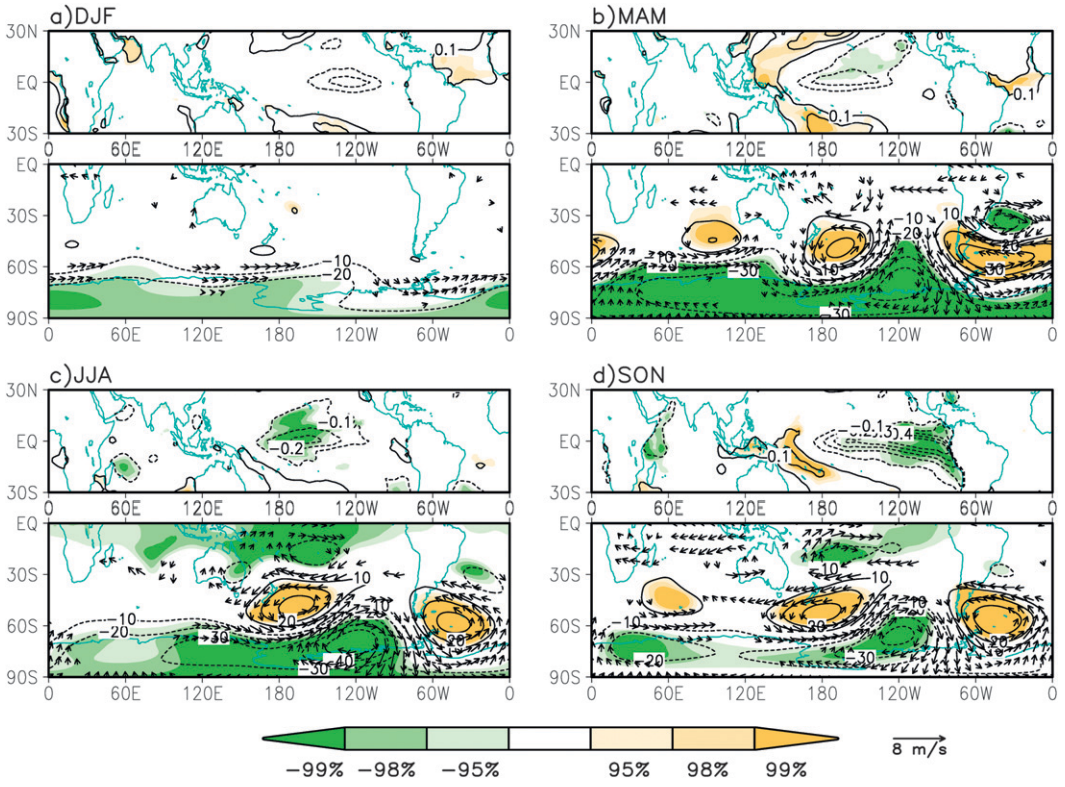

FIG. 4. Regression of seasonal mean APT times series against climate variables: (top) tropical SST (contour interval of 0.1°C) and (bottom) SH geopotential height (contour interval of 10 m) and wind (vector, m s^{-1}) at 200 hPa for (a) DJF, (b) MAM, (c) JJA, and (d) SON. Shading denotes regions in which correlation of APT with (top) SST or (bottom) Z200 is significant at or above the 95% confidence level. The (bottom) wind vectors, if either component is significantly related to the APT (above 95% confidence level), are displayed.

of each field. The corresponding squared singular value represents the squared covariance fraction and indicates the relative importance of that pair of vectors in relationship to the total covariance in the two fields. The expansion coefficients obtained by projecting the singular vectors onto the original data fields depicts the temporal variation of the spatial patterns. We also use this method to capture the dominant coupled modes between the sea ice cover in the AP and tropical SST.

c. *Model*

The general circulation modeling results presented in this study are based on two experiments with the ECHAM4.6 atmospheric general circulation model (Roeckner et al. 1996), at horizontal resolution of T42 (~2.8° latitude × 2.8° longitude) with 19 vertical levels. In all experiments we couple the ECHAM4.6 to a slab ocean (Manabe and Stouffer 1980). In the slab model, the ocean is represented by a horizontal grid of points that are slabs of water of uniform specified depth (50 m). The ocean temperature at each grid point is affected only by heat exchange across the air–sea interfaces. There is no direct communication between adjacent ocean grid points, nor is there any representation of the deep ocean. In addition, a set of specified surface flux adjustments are developed and added to the slab model's temperature tendency equation at each time step in order to maintain a seasonal cycle of ocean temperatures that is as close as possible to present-day conditions.

3. Interannual variability of the AP temperature

Examination of geopotential height fields shows that when temperature varies coherently across the AP, as measured by the APT time series, this variability is associated with a prominent wave train structure, with anomalous low and high 200-hPa geopotential height (Z200) to the west and east of the AP, respectively (Fig. 4). This local dipolelike circulation pattern has been called the Antarctic dipole (Liu et al. 2002), a leading interannually varying signal of circulation in the AP region. The wave train pattern associated with the Antarctic dipole appears in all seasons except summer. The vertical structure of the geopotential height anomalies follows the

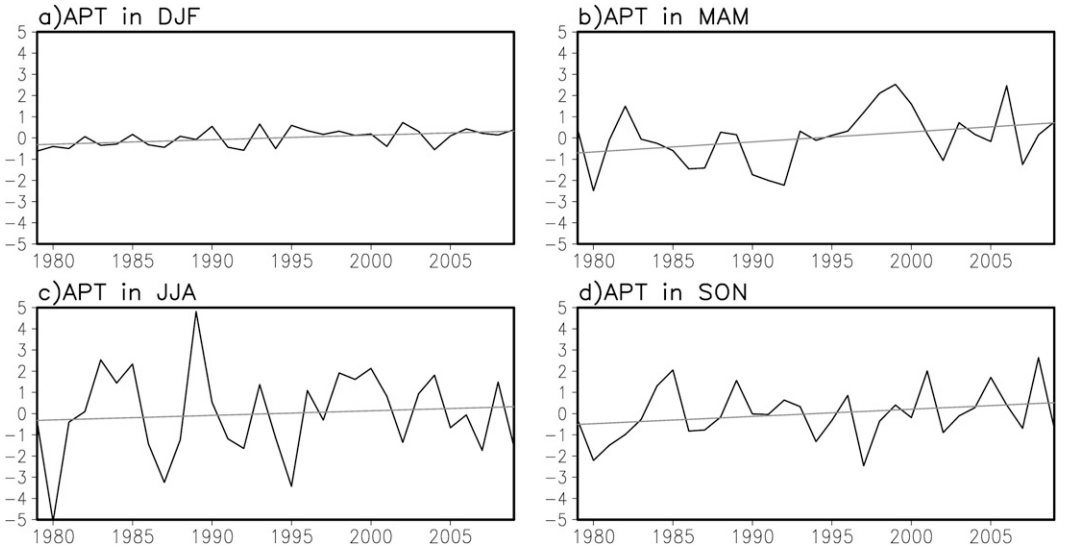

FIG. 5. Seasonal mean APT for (a) DJF, (b) MAM, (c) JJA, and (d) SON. Note that the upward trend (gray line) in DJF and MAM is significant at the 95% and 90% confidence level, respectively, by the Mann–Kendall test (Kendall 1955) and the trend-to-noise ratio test (Wilks 1995). The trends in JJA and SON are not significant.

classic pattern of a tropically forced Rossby wave train, baroclinic in the tropics, but barotropic elsewhere (Gill 1980). Consistent with this interpretation, the APT time series is significantly correlated with SST variability in the tropical and subtropical Pacific (Fig. 4). Locally, the northwesterly flow sandwiched between the low and high geopotential height anomalies favors strong heat transport from midlatitudes to the AP region. Temperature changes on the AP are thus intimately related to the large-scale northwesterly winds in fall (MAM) through spring (SON), which are in turn driven by the tropically forced Rossby wave train. In contrast, during austral summer the relationship between the APT (or W-APT and E-APT) and large-scale SH circulation is weak.

The seasonal character of the statistical relationships among geopotential height, SST anomalies, and AP temperatures may be understood in terms of the underlying dynamics that give rise to tropically forced Rossby wave trains. Although the pattern and location of the tropical SST anomaly associated with APT varies by season, in all three seasons during which the Rossby wave patterns appears (MAM, JJA, and SON), there is a strong meridional gradient of potential vorticity associated with the upper level subtropical jet to the east of Australia.

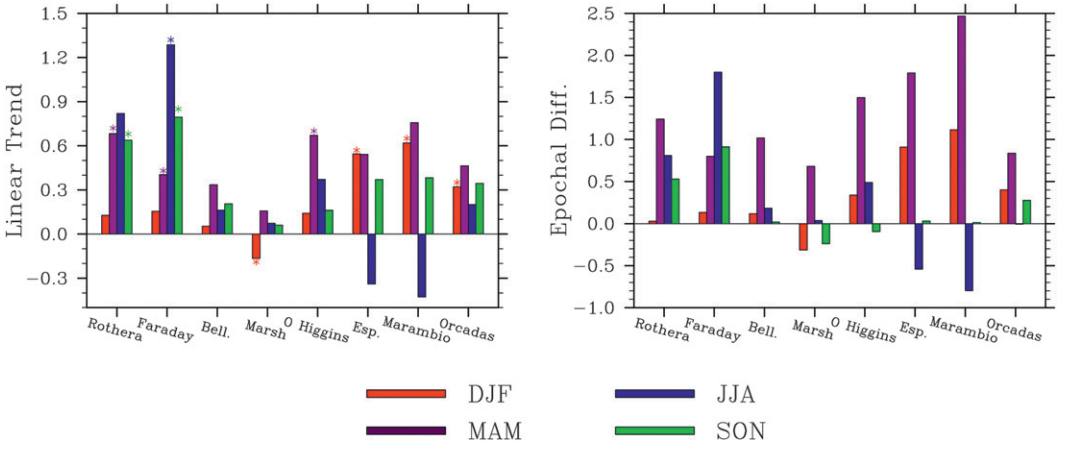

FIG. 6. (left) Linear trend (°C decade^{-1}) of 31 yr (1979–2009) seasonal mean surface temperature at each station for each season. (right) Epochal difference (1994–2009 minus 1979–93) of seasonal mean surface temperature at each station. In the top panel, the significant trends (above the 95% confidence level) are denoted by an asterisk.

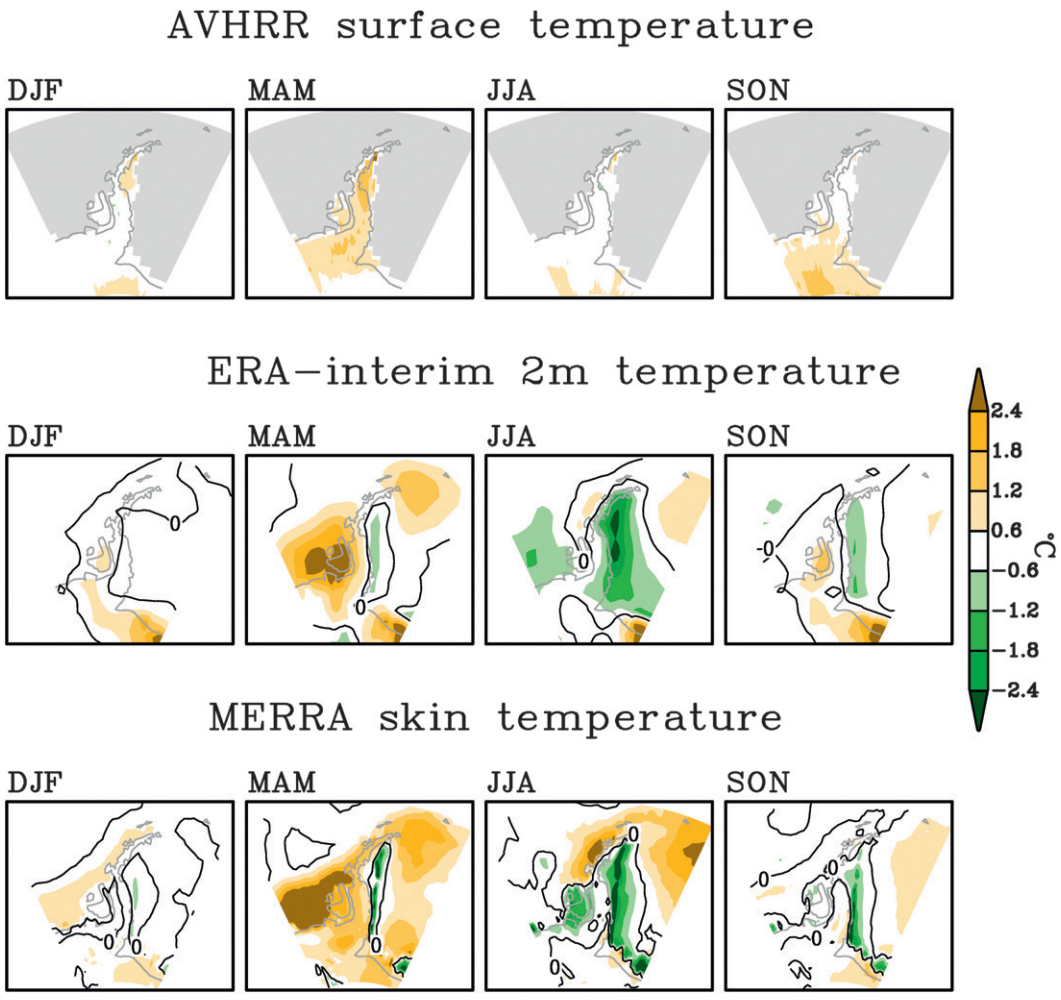

FIG. 7. Epochal difference (later period − early period) of seasonal mean surface air temperature in (top) AVHRR (land only), (middle) ERA-Interim, and (bottom) MERRA from DJF to SON. For AVHRR, the early period is 1982–93 and the later period is 1994–2006. The gray area indicates a region of no records. For ERA-Interim and MERRA, the early period is 1979–93 and the later period is 1994–2009.

This gradient acts as an amplifier to enhanced tropical forcing (Renwick and Revell 1999; Lachlan-Cope and Connolley 2006; Ding et al. 2012), which can be associated with a variety of SST anomaly patterns in the tropics and subtropics. In contrast, in summer [December–February (DJF)] the subtropical jet is normally weak or absent, and the connection between the AP and tropical SST variability is reduced.

4. Trend of the AP temperature

Trends in AP temperature, like the interannual variability, exhibit seasonality in both magnitude and spatial coherence. There is significant warming observed in summer and fall, but not in winter or spring (Fig. 5). Although the mean fall warming, as measured by the APT time series, is only marginally significant (93% confidence level), it occurs at all stations, and it is significant at 95% confidence at three of the eight stations (Fig. 6). In contrast, the summer warming, which has been attributed to the SAM trend (Thompson and Solomon 2002; Gillett et al. 2006; Marshall et al. 2006; Marshall 2007), mainly reflects the warming from the east side of the AP. In winter (JJA) and spring (SON), warming is seen primarily at just two stations (Faraday/Vernadsky and Rothera) on the west side (Fig. 6). It is thus only during the fall season that widespread warming of the entire peninsula is observed in the last few decades. This inference from the weather station data is supported by surface temperature data from satellite thermal infrared sensors, and by ERA-Interim and MERRA. The common feature of all three datasets indicates that the entire

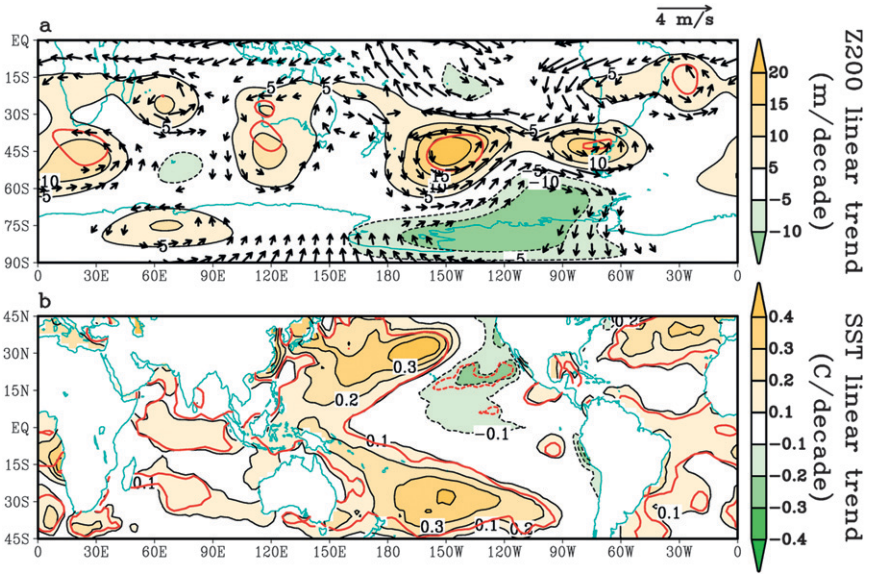

FIG. 8. Linear trend of austral fall tropical SST and SH circulation from 1979 to 2009. (a) Trend of SH 200-hPa geopotential height (color shading) and winds (vectors, displayed if either component is $>0.5\,\mathrm{m\,s^{-1}\,decade^{-1}}$) from ERA-Interim and (b) tropical SST from ERSSTv3. The significant trends in Z200 and SST (above the 95% confidence level) are enclosed by the red contours.

AP region has warmed significantly in fall, but not in the other three seasons (Fig. 7). The warming of Faraday/Vernadsky and Rothera in JJA and SON appears to represent only a local signal, rather than a peninsula-wide trend. Another interesting feature in MAM is that a very narrow cooling band is offshore of the east coast of the AP and this cooling band can also be seen in the other three seasons. But, to the first order, the entire AP region is only greatly warmed in MAM.

a. Tropical connection of the AP warming in fall

The peninsula-wide warming trend in fall can be related directly to tropically forced changes in the SH circulation over the last three decades. In particular, the SH circulation trend in fall is characterized by a wave train pattern in the Pacific sector (Fig. 8a), similar to that seen in the interannual variability from the tropical central Pacific to the AP (Fig. 4b). An increasing anomalous low circulation over the Amundsen Sea signifies an increasing trend of northwesterly flow and stronger heat transport from the midlatitudes to the AP. The decreasing trend of 200-hPa geopotential height over the Amundsen Sea is only significant at 80% confidence level as a result of a very high interannual variability there (Connolley 1997; Ding et al. 2012). Tropical Pacific SST in MAM experienced a significant change in the last 31 years (Fig. 8b), with significant warming in the western Pacific extending northeast and southeast into the subtropics.

Our inference that the spatially coherent trend in AP temperature in austral fall is associated with a trend in tropical SST is further supported by MCA. We use MCA to capture the dominant coupled modes between surface temperature on the AP (ERA-Interim; 60°–75°S, 79.5°–52.5°W) and tropical SST (30°N–30°S). The resulting SST pattern (SST mode 1) is similar to the simple SST trend in the last three decades shown in Fig. 8b, and is closely associated with a pattern of increasing surface temperature across the entire AP (AP mode 1; Fig. 9). This leading coupled pattern explains 70% of the covariability. The time series associated with these two modes are significantly correlated (correlation = 0.67) and both show a coherent upward trend in the last 31 years (Fig. 9c). The leading mode of AP temperature is very similar to the pattern of the AP warming trend in MAM (Fig. 7) and its time series is highly correlated with the APT time series (correlation = 0.9), and its increasing trend is significant at 99% confidence level.

Correlation of the time series of both the SST or AP temperature modes from the MCA with geopotential heights shows a wave train pattern that closely resembles the actual circulation trend in the last 31 years (Fig. 9d), indicating that this circulation pattern plays a key role in linking the tropics with peninsula-wide warming on both interannual and longer time scales. These results do not depend on whether the data are detrended prior to conducting the MCA calculation. Thus, the same physics that relates AP temperature to tropical SST on interannual

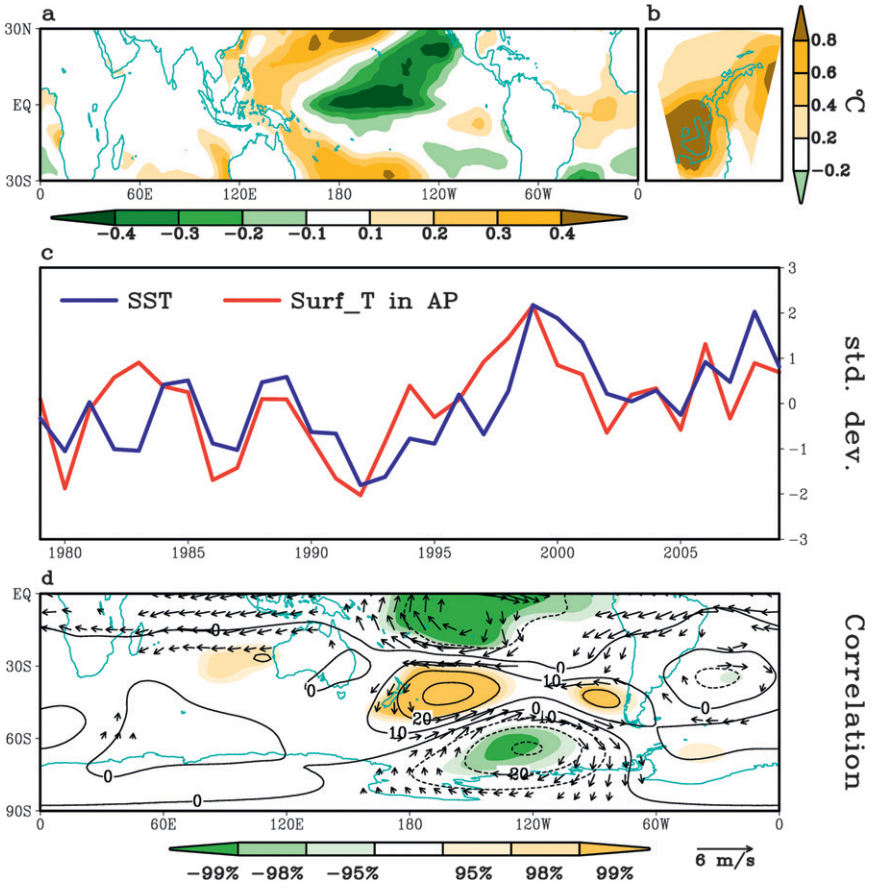

FIG. 9. Principal modes of covarying tropical SST and AP surface temperature in austral fall. MCA results for MAM 1979–2009 tropical (30°S–30°N) SST and surface air temperature in the AP. (a) Mode 1 tropical SST (shading interval 0.1°C) and (b) mode 1 surface temperature in the AP (shading interval 0.2°C). (c) Mode 1 expansion coefficient of the SST (blue) and surface air temperature in the AP (red). (d) Regression of the MCA mode 1 SST times series against ERA-Interim geopotential height (contour interval of 10 m) and winds (vector, $m\,s^{-1}$) at 200 hPa. Amplitudes in (a) and (b) are scaled by one std dev of the corresponding time series in (c). In (d), shading denotes regions in which correlation of MCA mode 1 SST time series with Z200 is significant at or above the 95% confidence level. The wind vectors are displayed if either component is significantly related to the MCA mode 1 SST times series (above the 95% confidence level).

time scales also appears to account for the significant trend of AP temperature in austral fall. Additional MCA analysis for pre-1979 period (1958–78) between the AP surface temperature from the 40-yr ECMWF Re-Analysis (ERA-40; Uppala et al. 2005) and tropical SST from ERSSTv3 still show a very similar coupled pattern in austral fall, suggesting a stable covarying relationship between the tropical SST and AP temperature in the last 50 years.

Temperature variation on the AP is closely tied to local sea ice conditions (Marshall et al. 2002; Jacobs and Comiso 1997; Turner et al. 2005). The APT times series is closely associated with sea ice conditions in the adjacent ocean on the interannual time scale throughout the year (Fig. 10), and the greatest decrease of sea ice cover off the west coast occurs in fall (Turner et al. 2009) (Fig. 11). In winter and spring, the sea ice decrease is largely restricted to the coast of the northwest and northeast peninsula. A similar MCA analysis between tropical SST (30°N–30°S) and sea ice in the peninsula region (HADISST; 60°–75°S, 79.5°–52.5°W) suggests that the same tropical SST trend that is related to AP temperature change in MAM also favors declining sea ice along the west coast of the peninsula region, especially over the Bellingshausen Sea (Fig. 12), where the largest decreasing trend of sea ice is seen in the last 31 years (Fig. 11). The tropically forced circulation change is associated with onshore wind over the Bellingshausen Sea,

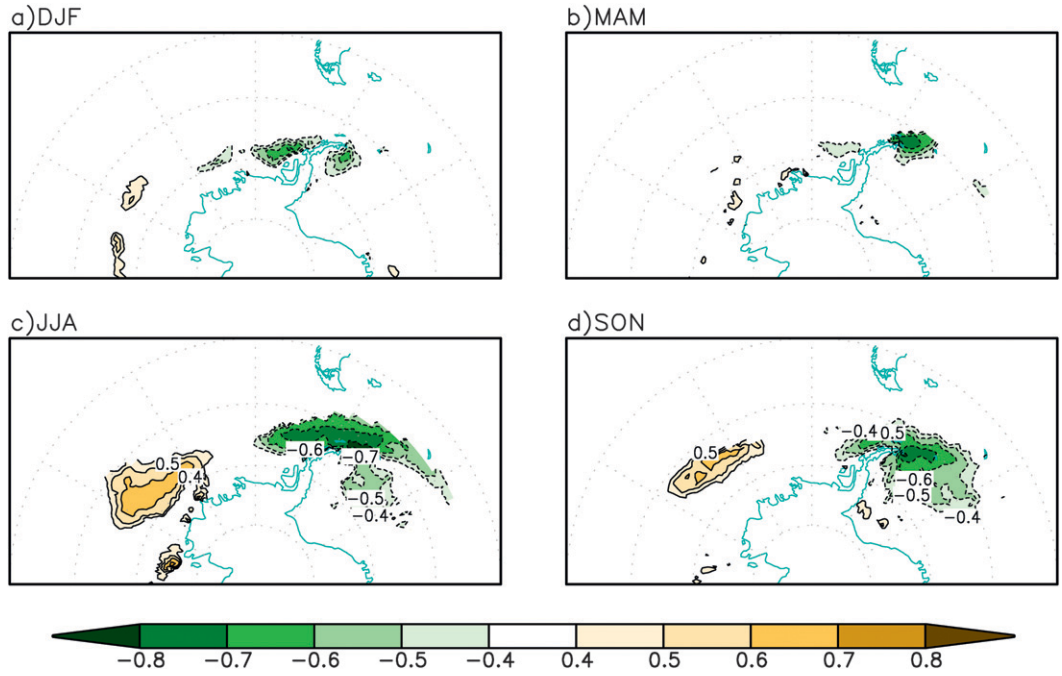

FIG. 10. Correlation of seasonal mean APT with sea ice concentration in the corresponding season for (a) DJF, (b) MAM, (c) JJA, and (d) SON. Only significant correlations (above the 98% confidence level: ±0.40) are displayed.

which provides favorable dynamical conditions for the movement of sea ice toward the coast (decreasing sea ice concentration) as well as favorable conditions for the melting of the sea ice by warm air advection (Harangozo 2000; Stammerjohn et al. 2008).

b. Model evidence of tropical connection of the AP warming in fall

To further examine the inferred causal relationship between tropical SST forcing and temperature variability

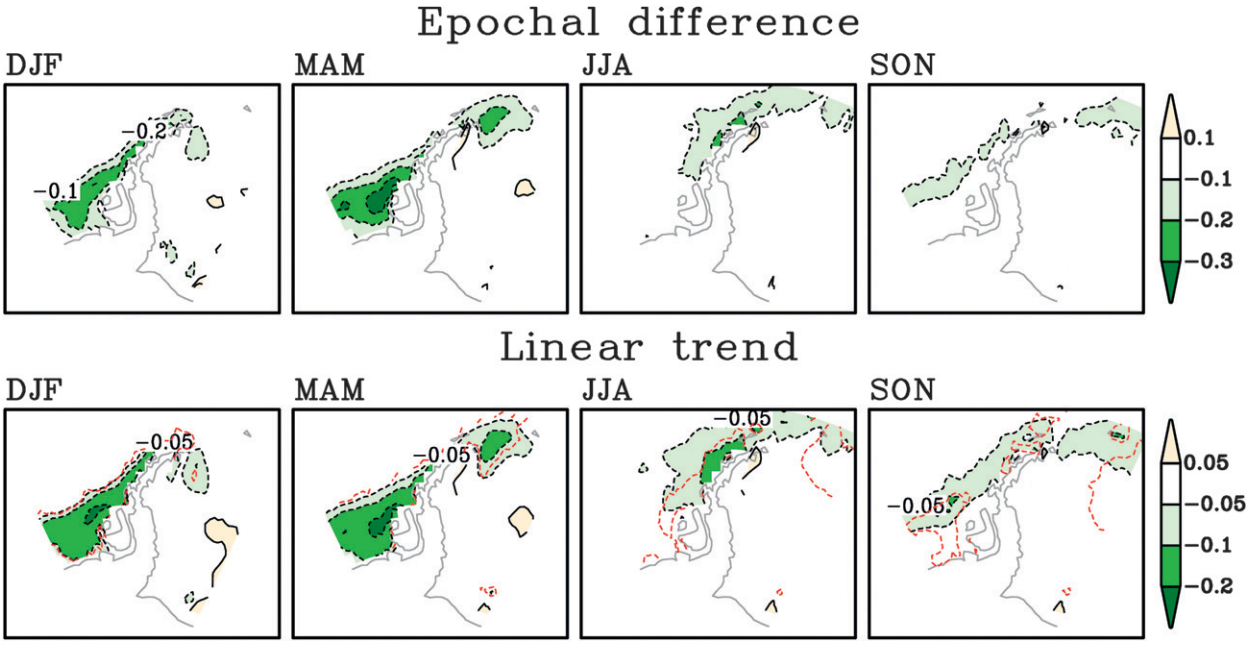

FIG. 11. (top) Epochal difference (1994–2009 minus 1979–93) of seasonal mean sea ice concentration in HadISST from DJF to SON. (bottom) Linear trend (fractional change per decade) of seasonal mean sea ice concentration in HadISST from DJF to SON since 1979–2009. In the bottom panel, the significant trends (above the 95% confidence level) are enclosed by red dashed contours.

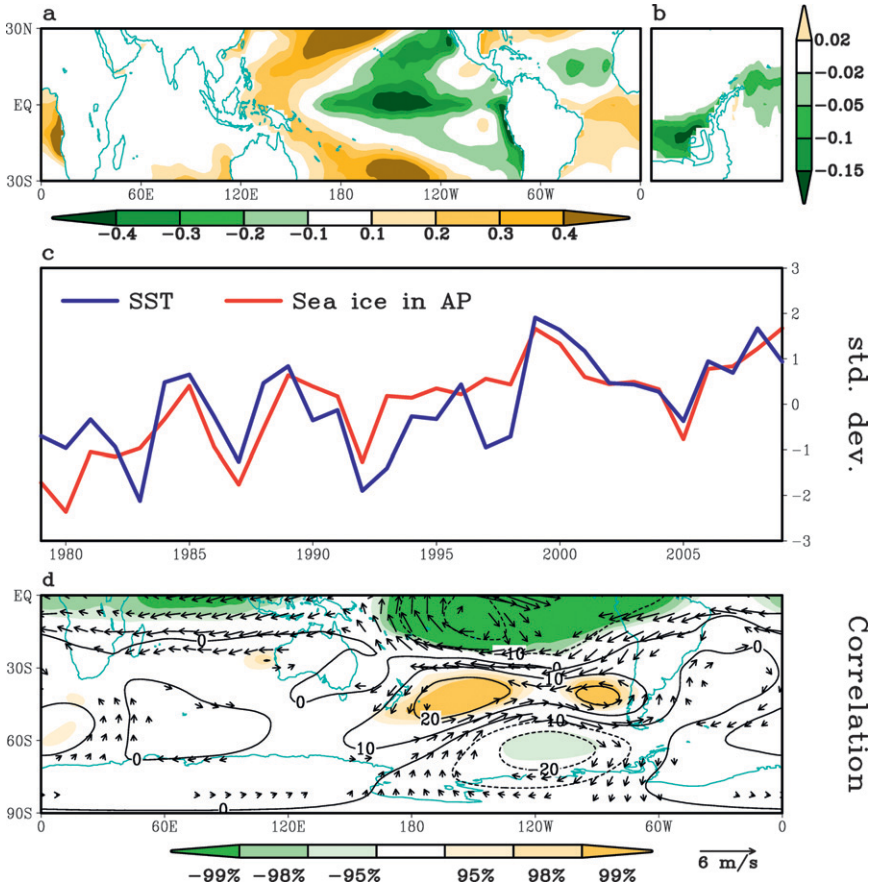

FIG. 12. MCA results for MAM 1979–2009 tropical (30°S–30°N) SST and sea ice concentration in the AP region. (a) Mode 1 tropical SST (shading interval 0.1°C), (b) mode 1 sea ice concentration, (c) mode 1 expansion coefficient of the SST (blue) and sea ice concentration (red), (d) regression of the MCA mode 1 SST times series against ERA-Interim geopotential height (contour interval of 10 m) and winds (vector, m s^{-1}) at 200 hPa. Amplitudes in (a) and (b) are scaled by one std dev of the corresponding time series in (c). In (d), shading denotes regions in which correlation of MCA mode 1 SST time series with Z200 is significant at or above the 95% confidence level. The wind vectors are displayed if either component is significantly related to the MCA mode 1 SST times series (above the 95% confidence level). This leading coupled pattern explains 80% of the covariability. The time series associated with these two modes are significantly correlated ($r = 0.73$) and both show a coherent significant (above the 95% confidence level) upward trend in the last 31 years.

in the AP during austral fall, we use an atmospheric general circulation model (GCM) forced by observed SSTs changes during the 1979–2009 period in the tropics only; in the extratropics, the atmosphere is coupled to a slab ocean. Thus, the high-latitude circulation change in this experiment is by construction resulting from the tropical forcing. Ten members run with different atmospheric initial conditions are used to obtain a reliable response. This experiment produces a very similar circulation trend pattern in the SH high latitude in fall, with a tropically forced northwesterly flow impinging on the west coast of the AP (Fig. 13), consistent with observations. The simulated MAM 200-hPa geopotential height variability in the Amundsen Sea, which is the key system to influence surface temperature in the AP, show a strong connection (correlation = −0.72) with the observed SST trend in the tropics (Fig. 13c). The simulated warming rate on the AP is 0.4°C decade^{-1}, in good agreement with observations. While the warming over the tip of peninsula seen in the observations is not captured, this area is actually misrepresented as an oceanic grid at the T42 model resolution used. Given the very reasonable simulation of high-latitude circulation trend and widespread warming across the AP associated with the observed SST variability, these model results add further evidence that tropical SST forcing has played a dominant role in warming the AP.

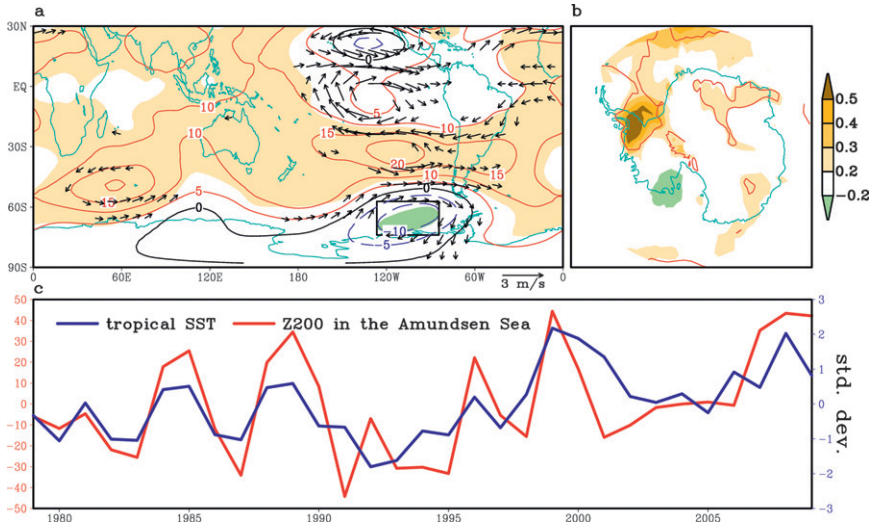

FIG. 13. Linear trend in MAM of (a) SH geopotential height (contour, 5 m decade^{-1}) and winds at 200 hPa (vectors, displayed if either component is >0.5 m s^{-1} decade^{-1}) and (b) surface temperature (°C decade^{-1}) in Antarctica from 31-yr simulation of ECHAM run forced by observed SST (1979–2009) in the tropics. In the extratropics, the atmosphere is coupled to a slab ocean model. (c) Simulated MAM Z200 anomalies averaged over the Amundsen Sea (74.0°–57.0°S, 125.0°–85.0°W), denoted as a black box in (a) from 1979 to 2009 (red curve, sign is reversed for the simplicity of the comparison) and observed mode 1 expansion coefficient of tropical SST in MCA analysis (blue curve from Fig. 9c). The correlation between the two curves is 0.72. In (a), the significant trends of simulated Z200 (above the 95% confidence level) are denoted by color shading. In (b), the significant trends of simulated surface temperature (above 95% confidence level) are enclosed by the red contours.

c. *Winter and spring warming in the western AP*

During austral winter and spring, the circulation trend over the AP is governed by strong easterly and southerly wind anomalies (Fig. 14), which cannot efficiently warm the region. This is the possible reason why the warming trends are significantly less widespread in these seasons (Figs. 6 and 7). However, a significant warming trend is still observed on west coast of the AP, especially over Faraday/Vernadsky and Rothera station (Fig. 6), which may be forced by a reduction of sea ice adjacent to the station (Jacobs and Comiso 1997). Although the sea ice reduction along the west coast of the AP in these two seasons cannot be readily explained by the large-scale circulation change, it is possible that the significant sea ice decline in fall persists into the subsequent winter and spring (Harangozo 2000; Stammerjohn et al. 2008). To test this idea, the mode 1 expansion coefficient of sea ice obtained from MCA analysis between MAM tropical SST and sea ice concentration in the peninsula region (Fig. 12) are used to capture tropical forcing-related sea ice variability in the AP region in fall. This time series characterizes well the total sea ice variability along the west coast in fall (Fig. 15a). The lag correlation between this time series with sea ice in the following two seasons suggests that the regional sea ice anomalies in fall persist to JJA and SON along the west coast of the peninsula, but with a slow eastward advection, resulting in sea ice reduction adjacent to Faraday/Vernadsky and Rothera (Fig. 15). The seasonally drifting pattern of regional sea ice anomalies is very similar to the trend pattern in winter and spring (Fig. 11). The time series of MAM sea ice variability also shows a significant correlation with JJA and SON station temperature over Faraday/Vernadsky and Rothera (Table 1). Thus, the sea ice decline in winter and spring that accounts for the warming trend in Faraday/Vernadsky and Rothera in those seasons (Jacobs and Comiso 1997) appears to be related to the sea ice trend in fall.

5. Discussion

Examination of the seasonal temperature variability across the peninsula shows that during all seasons except summer, the most important large-scale forcing of temperature variability on the AP is the extratropical Rossby wave train associated with tropical Pacific sea surface temperature anomalies. In the most recent three decades, austral fall is the only season in which a significant, spatially extensive warming trend occurs on the AP. This warming trend is associated with a significant reduction of

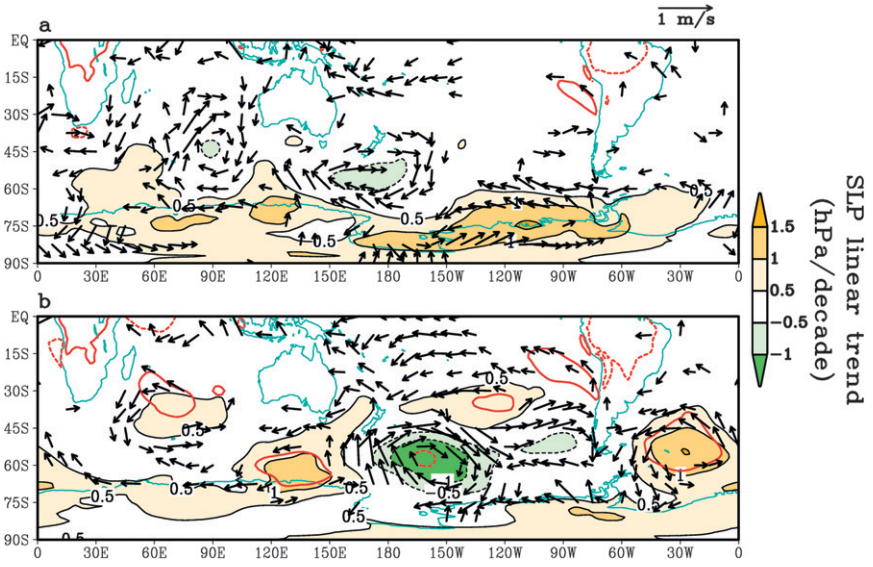

FIG. 14. Linear trend of SH sea level pressure (shading, hPa decade^{-1}) and winds at 10 m (vectors, displayed if either component is >0.2 m s^{-1} decade^{-1}) for the 1979–2009 period from ERA-Interim during austral (a) winter (JJA) and (b) spring (SON). The significant trends of SLP (above the 95% confidence level) are enclosed by the red contours.

sea ice off the west coast. Both appear to be primarily a response to a tropically forced atmospheric Rossby wave train. Because the sea ice reduction along the west coast in austral fall can persist for one to two seasons but drifts westward, the warming trends in winter and spring at Faraday/Vernadsky and Rothera on the western AP may also be related to the tropical forcing occurring in austral fall.

Our results have significant implications for understanding the role of anthropogenic forcing in driving recent temperature trends on the AP. Although the summertime warming of the eastern AP is widely attributed to anthropogenic radiative forcing of the SAM (Thompson and Solomon 2002; Gillett et al. 2006; Marshall et al. 2006; Marshall 2007), the same arguments do not apply to the widespread warming of the AP in fall, nor to the significant warming of the west coast in winter and spring (Marshall et al. 2004). We note that although regression of APT with upper-level circulation bears some resemblance to the SAM pattern in MAM (Fig. 4b), and correlation between the SAM index and the APT suggests a relationship at interannual time scales, this is not the case for the trend (Fig. 8a). Previous work on the recent trend in the SAM index has largely focused on summer during which the SAM trend has been statistically significant. In other three seasons, the trend in the

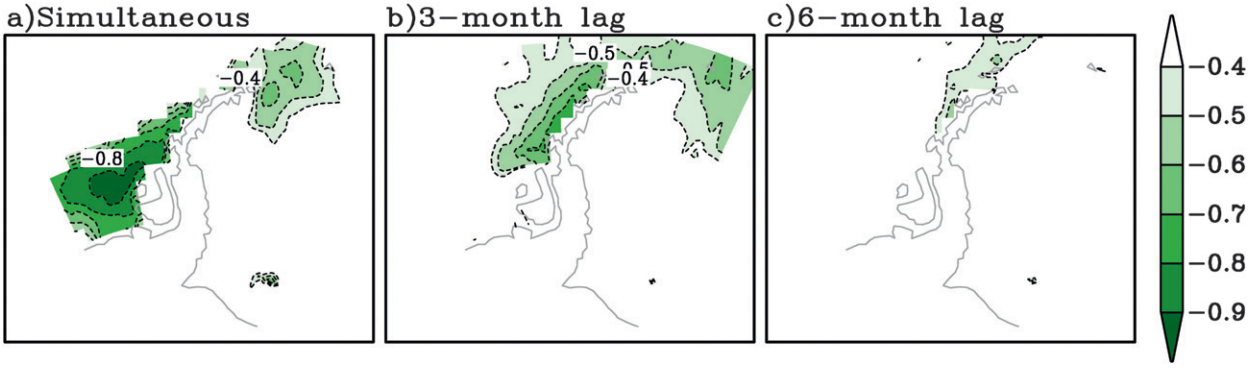

FIG. 15. (a) Spatial pattern of simultaneous correlation between MAM mode 1 expansion coefficient of sea ice concentration in the peninsula region (red curve in Fig. 12c) and MAM sea ice anomalies. (b) The 3-month lag correlation between the same MAM expansion coefficient of sea ice and JJA sea ice anomalies. (c) The 6-month lag correlation between the same MAM expansion coefficient of sea ice and SON sea ice anomalies. Only significant correlations (above the 98% confidence level: ±0.40) are displayed.

TABLE 1. Correlation of JJA and SON temperatures at Faraday/Vernadsky and Rothera with time series of MAM sea ice variability in the AP region obtained from MCA analysis between MAM tropical SST and sea ice concentration in the peninsula region (red curve of Fig. 12c). The correlation for detrended data is given in parentheses. The correlation significant at the 95% confidence is about ±0.35 for 31 years of data.

	JJA		SON	
	Faraday/Vernadsky	Rothera	Faraday/Vernadsky	Rothera
MAM sea ice	0.73 (0.67)	0.60 (0.64)	0.56 (0.35)	0.48 (0.33)

SAM is weaker, and the link with ozone or greenhouse gas forcing is much more equivocal (Marshall et al. 2004; Fogt et al. 2009; Sigmond and Fyfe 2010). Furthermore, the SAM component over the Pacific sector is strongly related to tropical forcing (Ding et al. 2012). Thus, the statistical connection between the SAM and APT does not contradict the idea that APT variability is strongly related to tropical dynamics.

We emphasize that the ECHAM4.6 model used in this paper, when run with a slab ocean and observed ozone and CO_2 forcing, captures the main features of observed geopotential height changes (i.e., the SAM trend) in DJF, as has been found with other models (Thompson and Solomon 2002; Gillett and Thompson 2003; Marshall et al. 2004; Shindell and Schmidt 2004; Miller et al. 2006; Arblaster and Meehl 2006; Fogt et al. 2009; Thompson et al. 2011). In the other seasons, a direct response to radiative forcing is clearly inadequate to explain the observed circulation patterns in the peninsula region (Fig. 16). While a nonannular circulation pattern similar

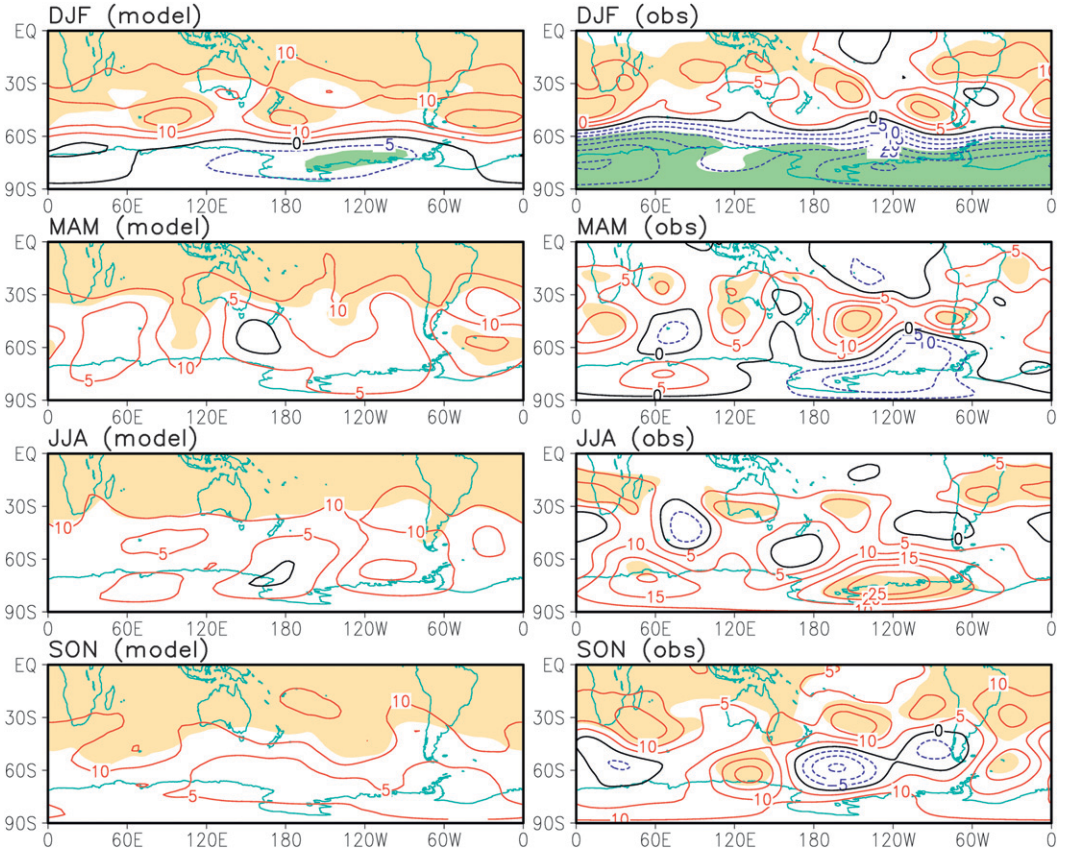

FIG. 16. Linear trend of SH Z200 (contour, 5 m decade^{-1}) in each season from (left) 31-yr ECHAM4.6 model response and (right) 1979–2009 period of ERA-Interim observations. The model is forced by observed 31-yr (1979–2009) CO_2 and ozone forcing. In the lower boundary, the atmosphere is coupled to a slab ocean model. Ten members run with different atmospheric initial condition are used to obtain a reliable response. The mean of the 10-member ensemble is shown here. The significant trends of simulated and observed Z200 (above 95% confidence level) are denoted by color shading.

to the observed trend in MAM has been produced in one atmospheric model in response to ozone forcing (Turner et al. 2009), our results suggest that the response should be quite sensitive to the SST field. Tropical Pacific SSTs are a key forcing of nonannular features in the SH circulation (Ding et al. 2012), and as we have shown here, the observed circulation changes and AP temperatures covary strongly with observed tropical SST. This does not rule out an anthropogenic forcing of AP temperature, because it is possible that the tropical SST changes are themselves a response to radiative forcing. However, at least some modeling results suggest that the recent SST change in the tropical Pacific is mainly attributable to natural variability (Yeh et al. 2012).

How the tropical Pacific response to the anthropogenic forcing is a subject of considerable uncertainty: the atmospheric dynamics favor an El Niño–like response, while the oceanic dynamic favor a La Niña–like response (Vecchi et al. 2008; Collins et al. 2010). Furthermore, it is clear that there is strong natural SST variability in the tropical Pacific on decadal time scales (Meyers et al. 1999; Di Lorenzo et al. 2010). Thus, future projections of how tropical Pacific low-frequency SST variability will change in response to both continued anthropogenic radiative forcing and natural interdecadal variability represent a significant source of uncertainty of projections of temperature change in the AP.

Acknowledgments. Q.D. and E.J.S. were supported by the U.S. National Science Foundation, Grant OPP-0837988. We thank G. Hoffman for providing the code for ECHAM4.6.

REFERENCES

Arblaster, J. M., and G. A. Meehl, 2006: Contributions of external forcings to southern annular mode trends. *J. Climate,* **19,** 2896–2905.

Bracegirdle, T. J., and G. J. Marshall, 2012: The reliability of Antarctic tropospheric pressure and temperature in the latest global reanalyses. *J. Climate,* **25,** 7138–7146.

Bretherton, C. S., C. Smith, and J. M. Wallace, 1992: An intercomparison of methods for finding coupled patterns in climate data. *J. Climate,* **5,** 541–560.

Bromwich, D. H., R. L. Fogt, K. I. Hodges, and J. E. Walsh, 2007: A tropospheric assessment of the ERA-40, NCEP, and JRA-25 global reanalyses in the polar regions. *J. Geophys. Res.,* **112,** D10111, doi:10.1029/2006JD007859.

——, J. P. Nicolas, A. J. Monaghan, M. A. Lazzara, L. M. Keller, G. A. Weidner, and A. B. Wilson, 2013: Central West Antarctica among the most rapidly warming regions on Earth. *Nat. Geosci.,* **6,** 139–145.

Chapman, W. L., and J. E. Walsh, 2007: A synthesis of Antarctic temperatures. *J. Climate,* **20,** 4096–4117.

Collins, M., and Coauthors, 2010: The impact of global warming on the tropical Pacific Ocean and El Niño. *Nat. Geosci.,* **3,** 391–397.

Comiso, J. C., 2000: Variability and trends in Antarctic surface temperatures from in situ and satellite infrared measurements. *J. Climate,* **13,** 1674–1696.

Connolley, W. M., 1997: Variability in annual mean circulation in southern high latitudes. *Climate Dyn.,* **13,** 745–756.

Dee, D. P., and Coauthors, 2011: The ERA-Interim reanalysis: Configuration and performance of the data assimilation system. *Quart. J. Roy. Meteor. Soc.,* **137,** 553–597.

Di Lorenzo, E., K. M. Cobb, J. C. Furtado, N. Schneider, B. T. Anderson, A. Bracco, M. A. Alexander, and D. J. Vimont, 2010: Central Pacific El Niño and decadal climate change in the North Pacific Ocean. *Nat. Geosci.,* **3,** 762–765.

Ding, Q., E. J. Steig, D. S. Battisti, and M. Küettel, 2011: Winter warming in West Antarctica caused by central tropical Pacific warming. *Nat. Geosci.,* **4,** 398–403.

——, ——, ——, and J. M. Wallace, 2012: Influence of the tropics on the southern annular mode. *J. Climate,* **25,** 6330–6363.

Fogt, R. L., and D. H. Bromwich, 2006: Decadal variability of the ENSO teleconnection to the high-latitude South Pacific governed by coupling with the southern annular mode. *J. Climate,* **19,** 979–997.

——, J. Perlwitz, A. J. Monaghan, D. H. Bromwich, J. M. Jones, and G. J. Marshall, 2009: Historical SAM variability. Part II: Twentieth-century variability and trends from reconstructions, observations, and the IPCC AR4 model. *J. Climate,* **22,** 5346–5365.

——, D. H. Bromwich, and K. M. Hines, 2011: Understanding the SAM influence on the South Pacific ENSO teleconnection. *Climate Dyn.,* **36,** 1555–1576.

——, A. J. Wovrosh, R. A. Langen, and I. Simmonds, 2012: The characteristic variability and connection to the underlying synoptic activity of the Amundsen–Bellingshausen Seas Low. *J. Geophys. Res.,* **117,** D07111, doi:10.1029/2011JD017337.

Gill, A. E., 1980: Some simple solutions for heat induced tropical circulation. *Quart. J. Roy. Meteor. Soc.,* **106,** 447–462.

Gillett, N. P., and D. W. J. Thompson, 2003: Simulation of recent Southern Hemisphere climate change. *Science,* **302,** 273–275.

——, T. D. Kell, and P. D. Jones, 2006: Regional climate impacts of the Southern Annular Mode. *Geophys. Res. Lett.,* **33,** L23704, doi:10.1029/2006GL027721.

Grassi, B., G. Redaelli, and G. Visconti, 2005: Simulation of Polar Antarctic trends: Influence of tropical SST. *Geophys. Res. Lett.,* **32,** L23806, doi:10.1029/2005GL023804.

Harangozo, S. A., 2000: A search for ENSO teleconnections in the west Antarctic Peninsula climate in austral winter. *Int. J. Climatol.,* **20,** 663–679.

Holland, P. R., and R. Kwok, 2012: Wind-driven trends in Antarctic sea ice drift. *Nat. Geosci.,* **5,** 872–875.

Jacobs, S. S., and J. C. Comiso, 1997: Climate variability in the Amundsen and Bellingshausen Seas. *J. Climate,* **10,** 697–709.

Karoly, D. J., 1989: Southern Hemisphere circulation features associated with El Niño–Southern Oscillation events. *J. Climate,* **2,** 1239–1252.

Kendall, M. G., 1955: *Rank Correlation Methods*. 2nd ed. Charles Griffin, 196 pp.

Lachlan-Cope, T. A., and W. Connolley, 2006: Teleconnections between the tropical Pacific and the Amundsen-Bellinghausens Sea: Role of the El Niño/Southern Oscillation. *J. Geophys. Res.,* **111,** D23101, doi:10.1029/2005JD006386.

Liu, J., X. Yuan, D. Rind, and D. G. Martinson, 2002: Mechanism study of the ENSO and southern high latitude climate teleconnections. *Geophys. Res. Lett.,* **29,** 1679, doi:10.1029/2002GL015143.

——, J. A. Curry, and D. G. Martinson, 2004: Interpretation of recent Antarctic sea ice variability. *Geophys. Res. Lett.,* **31,** L02205, doi:10.1029/2003GL018732.

Manabe, S., and R. J. Stouffer, 1980: Sensitivity of a global climate model to an increase of CO_2 concentration in the atmosphere. *J. Geophys. Res.,* **85** (C10), 5529–5554.

Marshall, G. J., 2007: Half-century seasonal relationships between the Southern Annular Mode and Antarctic temperatures. *Int. J. Climatol.,* **27,** 373–383.

——, and J. C. King, 1998: Southern hemisphere circulation anomalies associated with extreme Antarctic peninsula winter temperatures. *Geophys. Res. Lett.,* **25,** 2437–2440.

——, V. Lagun, and T. A. Lachlan-Cope, 2002: Changes in Antarctic Peninsula tropospheric temperatures from 1956–99: A synthesis of observations and reanalysis data. *Int. J. Climatol.,* **22,** 291–310.

——, P. A. Stott, J. Turner, W. M. Connolley, J. C. King, and T. A. Lachlan-Cope, 2004: Causes of exceptional atmospheric circulation changes in the Southern Hemisphere. *Geophys. Res. Lett.,* **31,** L14205, doi:10.1029/2004GL019952.

——, A. Orr, N. P. M. Van Lipzig, and J. C. King, 2006: The impact of changing Southern Hemisphere Annular Mode on Antarctic Peninsula summer temperatures. *J. Climate,* **19,** 5388–5404.

Meyers, S. D., J. J. O'Brien, and E. Thelin, 1999: Reconstruction of monthly SST in the tropical Pacific Ocean during 1868–1993 using adaptive climate basis functions. *Mon. Wea. Rev.,* **127,** 1599–1612.

Miller, R. L., G. A. Schmidt, and D. T. Shindell, 2006: Forced annular variations in the 20th century Intergovernmental Panel on Climate Change Fourth Assessment Report models. *J. Geophys. Res.,* **111,** D18101, doi:10.1029/2005JD006323.

Monaghan, A. J., and D. H. Bromwich, 2008: Advances in describing recent Antarctic climate variability. *Bull. Amer. Meteor. Soc.,* **89,** 1295–1306.

——, ——, W. Chapman, and J. C. Comiso, 2008: Recent variability and trends of Antarctic near-surface temperature. *J. Geophys. Res.,* **113,** D04105, doi:10.1029/2007JD009094.

Okumura, Y. M., D. Schneider, C. Deser, and R. Wilson, 2012: Decadal–interdecadal climate variability over Antarctica and linkages to the tropics: Analysis of ice core, instrumental, and tropical proxy data. *J. Climate,* **25,** 7421–7441.

Orr, A., G. J. Marshall, Julian C. R. Hunt, J. Sommeria, C.-G. Wang, N. P. M. Van Lipzig, Doug Cresswell, and J. C. King, 2008: Characteristics of summer airflow over the Antarctic Peninsula in response to recent strengthening of westerly circumpolar winds. *J. Atmos. Sci.,* **65,** 1396–1413.

Orsi, A. J., B. D. Cornuelle, and J. P. Severinghaus, 2012: Little Ice Age cold interval in West Antarctica: Evidence from borehole temperature at the West Antarctic Ice Sheet (WAIS) Divide. *Geophys. Res. Lett.,* **39,** L09710, doi:10.1029/2012GL051260.

Rayner, N. A., D. E. Parker, E. B. Horton, C. K. Folland, L. V. Alexander, D. P. Rowell, E. C. Kent, and A. Kaplan, 2003: Global analyses of sea surface temperature, sea ice, and night marine air temperature since the late nineteenth century. *J. Geophys. Res.,* **108,** 4407, doi:10.1029/2002JD002670.

Renwick, J. A., 2002: Southern Hemisphere circulation and relations with sea ice and sea surface temperature. *J. Climate,* **15,** 3058–3068.

——, and M. J. Revell, 1999: Blocking over the South Pacific and Rossby wave propagation. *Mon. Wea. Rev.,* **127,** 2233–2247.

Rienecker, M. M., and Coauthors, 2011: MERRA: NASA's Modern-Era Retrospective Analysis for Research and Applications. *J. Climate,* **24,** 3624–3648.

Roeckner, E., and Coauthors, 1996: The atmospheric general circulation model ECHAM4: Model description and simulation of present day climate. Max Planck Institut für Meteorologie Rep. 218, 90 pp.

Schneider, D. P., C. Deser, and Y. Okumura, 2012a: An assessment and interpretation of the observed warming of West Antarctica in the austral spring. *Climate Dyn.,* **38,** 323–347.

——, Y. Okumura, and C. Deser, 2012b: Observed Antarctic interannual climate variability and tropical linkages. *J. Climate,* **25,** 4048–4066.

Shindell, D. T., and G. A. Schmidt, 2004: Southern Hemisphere climate response to ozone changes and greenhouse gas increases. *Geophys. Res. Lett.,* **31,** L18209, doi:10.1029/2004GL020724.

Sigmond, M., and J. C. Fyfe, 2010: Has the ozone hole contributed to increased Antarctic sea ice extent? *Geophys. Res. Lett.,* **37,** L18502, doi:10.1029/2010GL044301.

Smith, T. M., R. W. Reynolds, T. C. Peterson, and J. Lawrimore, 2008: Improvements to NOAA's historical merged land–ocean surface temperature analysis (1880–2006). *J. Climate,* **21,** 2283–2296.

Stammerjohn, S. E., D. G. Martinson, R. C. Smith, X. Yuan, and D. Rind, 2008: Trends in Antarctic annual sea ice retreat and advance and their relation to El Niño–Southern Oscillation and Southern Annular Mode variability. *J. Geophys. Res.,* **113,** C03S90, doi:10.1029/2007JC004269.

Steig, E. J., and A. J. Orsi, 2013: The heat is on in Antarctica. *Nat. Geosci.,* **6,** 87–88.

——, D. P. Schneider, S. D. Rutherford, M. E. Mann, J. C. Comiso, and D. T. Shindell, 2009: Warming of the Antarctic ice-sheet surface since the 1957 International Geophysical Year. *Nature,* **457,** 459–462.

——, Q. Ding, D. S. Battisti, and A. Jenkins, 2012: Tropical forcing of circumpolar deep water inflow and outlet glacier thinning in the Amundsen Sea Embayment, West Antarctica. *Ann. Glaciol.,* **53,** 19–28.

Thompson, D. W. J., and J. M. Wallace, 2000: Annular modes in the extratropical circulation. Part I: Month-to-month variability. *J. Climate,* **13,** 1000–1016.

——, and S. Solomon, 2002: Interpretation of recent Southern Hemisphere climate change. *Science,* **296,** 895–899.

——, ——, P. J. Kushner, M. E. England, K. M. Grise, and D. J. Karoly, 2011: Signatures of the Antarctic ozone hole in Southern Hemisphere surface climate change. *Nat. Geosci.,* **4,** 741–749.

Trivelpiece, W. Z., J. T. Hinke, A. K. Miller, C. S. Reiss, S. G. Trivelpiece, and G. M. Watters, 2011: Variability in krill biomass links harvesting and climate warming to penguin population changes in Antarctica. *Proc. Natl. Acad. Sci. USA,* **108,** 7625–7628.

Turner, J., and Coauthors, 2005: Antarctic climate change during the last 50 years. *Int. J. Climatol.,* **25,** 279–294.

——, and Coauthors, 2009: Non-annular atmospheric circulation change induced by stratospheric ozone depletion and its role in the recent increase of Antarctic sea ice extent. *Geophys. Res. Lett.,* **36,** L08502, doi:10.1029/2009GL037524.

Uppala, S. M., and Coauthors, 2005: The ERA-40 Re-Analysis. *Quart. J. Roy. Meteor. Soc.,* **131,** 2961–3012.

Van den Broeke, M., 2005: Strong surface melting preceded collapse of Antarctic Peninsula ice shelf. *Geophys. Res. Lett.,* **32,** L12815, doi:10.1029/2005GL023247.

van Lipzig, N. P. M., G. J. Marshall, A. Orr, and J. C. King, 2008: The relationship between the Southern Hemisphere annular mode and Antarctic Peninsula summer temperatures: Analysis of a high-resolution model climatology. *J. Climate,* **21,** 1649–1668.

Vaughan, D. G., and Coauthors, 2003: Recent rapid regional climate warming on the Antarctic Peninsula. *Climate Change,* **60,** 243–274.

Vecchi, G. A., A. Clement, and B. J. Soden, 2008: Examining the Tropical Pacific's response to global warming. *Eos, Trans. Amer. Geophys. Union,* **89,** 81–83.

Wilks, D. S., 1995: *Statistical Methods in the Atmospheric Sciences: An Introduction*. Academic Press, 467 pp.

Yeh, S. W., Y. G. Ham, and J. Y. Lee, 2012: Changes in the tropical Pacific SST trend from CMIP3 to CMIP5 and its implication of ENSO. *J. Climate,* **25,** 7764–7771.

Yuan, X. J., 2004: ENSO-related impacts on Antarctic sea ice: A synthesis of phenomenon and mechanisms. *Antarct. Sci.,* **16,** 415–425.

——, and D. G. Martinson, 2000: Antarctic sea ice extent variability and its global connectivity. *J. Climate,* **13,** 1697–1717.